

# Analysis and Optimization of the Characteristics of a New IEC-GTO Thyristor\*

Wang Cailin<sup>†</sup> and Gao Yong

(Department of Electronic Engineering, Xi'an University of Technology, Xi'an 710048, China)

**Abstract:** Based on a short anode GTO structure (SA-GTO), a novel GTO structure called an injection efficiency controlled gate turn off thyristor (IEC-GTO) is proposed, in which the injection efficiency can be controlled via an additional thin oxide layer located in the short anode contact region. The forward blocking, conducting, and switching characteristics are analyzed and compared with an SA-GTO and conventional GTO. The results show that the IEC-GTO can obtain a better trade-off relation between on-state and turn-off characteristics. Additionally, the width of the oxide layer covering the anode region and the doping concentration of the anode region are optimized, the process feasibility is analyzed, and a realization scheme is given. The results show that the introduction of an oxide layer would not increase the complexity of process of the IEC-GTO.

**Key words:** power semiconductor devices; gate turn-off thyristor; injection efficiency

**EEACC:** 2560P; 2560L; 2560B

**CLC number:** TN34

**Document code:** A

**Article ID:** 0253-4177(2007)04-0484-06

## 1 Introduction

It is normally difficult to obtain high blocking voltage, low on-state voltage drop, and fast switching speed with the same design parameters for power semiconductor devices. Therefore the anode injection efficiency should be enhanced in the on state and weakened or ideally eliminated during turn-off. This can be achieved by the short anode structure in a gate turn-off thyristor (GTO)<sup>[1]</sup> or the transparent anode structure in a gate commutated thyristor (GCT)<sup>[2]</sup>. However, the short anode used in a GTO causes the gate trigger current and voltage drop to increase, and the transparent anode used in a GCT is a shallow junction and requires an additional n buffer layer, which complicates the fabrication process. In this paper, based on a short anode gate turn-off thyristor (SA-GTO), an injection efficiency controlled GTO (IEC-GTO) structure is presented, and its characteristics are analyzed and compared with those of an SA-GTO and conventional GTO. Also, the process feasibility is analyzed and a realization scheme is given.

## 2 Device structure and operation mechanism

The basic structures and equivalent circuits of IEC-GTO, SA-GTO, and GTO are shown in Fig. 1. Seen from Fig. 1(a), the IEC-GTO is very similar to an SA-GTO as shown in Fig. 1(b), in which the partial p<sup>+</sup> anode region is replaced by an n<sup>+</sup> short region. Comparatively, the n<sup>+</sup> region of an IEC-GTO is floating and isolated from the anode contact via a thin silicon dioxide layer, and the anode contact area of the IEC-GTO is lightly reduced. If the additional thin oxide layer is removed, the structure of the IEC-GTO is identical to that of an SA-GTO, and they have identical doping profiles and dimensions in other regions except for a slight decrease in anode contact area and doping concentration. The doping concentration of the p<sup>+</sup> anode region is expressed by  $N_A$ , and the width and thickness of oxide layer covered on the p<sup>+</sup> anode region as shown in Fig. 1(a) can be expressed by  $W_{ox}$  and  $Z_{ox}$ , respectively.

During the operation of an IEC-GTO, electrons in the n<sup>-</sup> base region drift toward the p<sup>+</sup> anode and the n<sup>+</sup> floating regions covered with

\* Project supported by the Outstanding Doctor Research Foundation and Research Plan of Xi'an University of Technology

<sup>†</sup> Corresponding author. Email: wangcailin@xaut.edu.cn

Received 28 September 2006, revised manuscript received 17 November 2006

©2007 Chinese Institute of Electronics

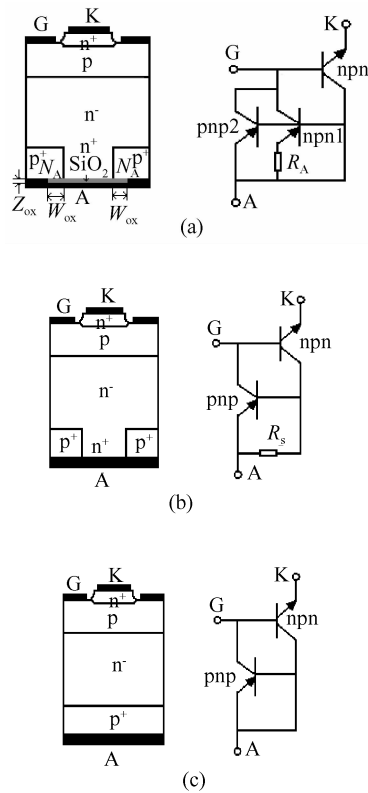


Fig. 1 Basic structures and equivalent circuits of IEC-GTO, SA-GTO, and conventional GTO (a) IEC-GTO; (b) SA-GTO; (c) Conventional GTO

oxide layer under an external positive voltage. Because of the thin oxide layer located at the anode, the electrons cannot be collected directly by the anode ohm contact, and they accumulate near the oxide layer, resulting in an increase of electron concentration in the  $n^-$  base and  $n^+$  floating regions and enabling the potential fall. In order to maintain electrical neutrality of the  $n^-$  base and  $n^+$  floating regions, the hole injection from the  $p^+$  anode to the  $n^-$  base region must be enhanced. Being similar to the injection enhanced gate transistor (IEGT)<sup>[3]</sup>, this is called the hole injection enhancement effect (IE-effect), and its intensity is related to the resistance of the anode region  $R_A$ .

$R_A$  is determined by the doping concentration and cross sectional area of the  $p^+$  anode region. Because the  $p^+$  anode region of the IEC-GTO has a narrow cross section and moderate doping,  $R_A$  is significant. The doping concentration in the  $n^+$  floating region is higher than that of the  $n^-$  base region. Thus the anode pnp transistor of an IEC-GTO can be taken as a two-emitter transistor,

i. e., the  $p^+$  anode,  $n^-$  base, and  $p$  base form pnp1 and the  $p^+$  anode,  $n^+$  floating,  $n^-$  base and  $p$  base form pnp2. Seen from the equivalent circuit of an IEC-GTO as shown in Fig. 1 (a), the emitter-base voltage drop of pnp2 transistor can be expressed as

$$V_{be(pnp2)} = V_{be(pnp1)} + R_A I_{A(pnp1)} \quad (1)$$

As a positive voltage is applied across the anode and cathode of the IEC-GTO, a low anode current  $I_A$  flows mainly through pnp1. With the increase of  $I_A$ , the voltage drop across  $R_A$  rises and  $V_{be(pnp1)}$  falls, causing the hole injection of pnp1 to fall and more current to flow through pnp2. pnp1 has higher hole injection efficiency than pnp2 because the  $n^-$  base region is adjacent to the  $p^+$  anode in pnp1 and pnp2 is a wide base transistor. Thus the anode injection efficiency of an IEC-GTO varies with  $I_A$ , and it is enhanced at low  $I_A$  and reduced at high  $I_A$ . This is helpful to improve the switching and on-state characteristics of IEC-GTO.

### 3 Analysis and optimal of characteristics

In order to evaluate the performance of an IEC-GTO, a structural model as shown in Fig. 1 (a) is set up, which is a profile along the cathode cell width,  $Z_{ox}$  is  $0.5\mu\text{m}$ , and  $W_{ox}$  is  $25\mu\text{m}$ . The surface doping concentration of the anode region  $N_{AS}$  is  $(3\sim 5) \times 10^{18}\text{cm}^{-3}$ . The other parameters are the same as those of an SA-GTO. Based on this model, the forward blocking, conducting, and switching characteristics of an IEC-GTO are simulated by MEDICI<sup>[4]</sup> and compared with those of an SA-GTO and conventional GTO.

#### 3.1 Forward blocking

The forward  $I$ - $V$  characteristics of an IEC-GTO, SA-GTO, and conventional GTO during blocking are simulated as shown in Fig. 2. Seen from this figure, the forward breakdown voltage of an IEC-GTO is the same as that of a conventional GTO and smaller than an SA-GTO, about 100V. This is because the current gain of the anode pnp transistor of an IEC-GTO for the hole IE-effect is very close to that of a conventional GTO, and higher than that of an SA-GTO, so the forward breakdown voltage affected by the cur-

rent gain of the pnp transistor falls slightly. This shows the forward blocking voltage of an IEC-GTO nearer that of an SA-GTO.

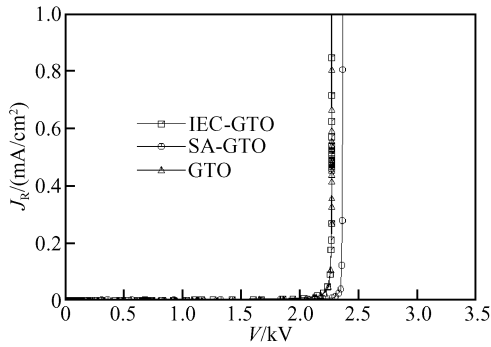


Fig. 2 Comparison of the  $I$ - $V$  characteristics of IEC-GTO, SA-GTO, and conventional GTO during blocking

### 3.2 Conducting

Firstly, a comparison of the carrier distributions of an IEC-GTO, SA-GTO, and conventional GTO during conduction along the profile of the  $n^+$  cathode region center is shown in Fig. 3, in

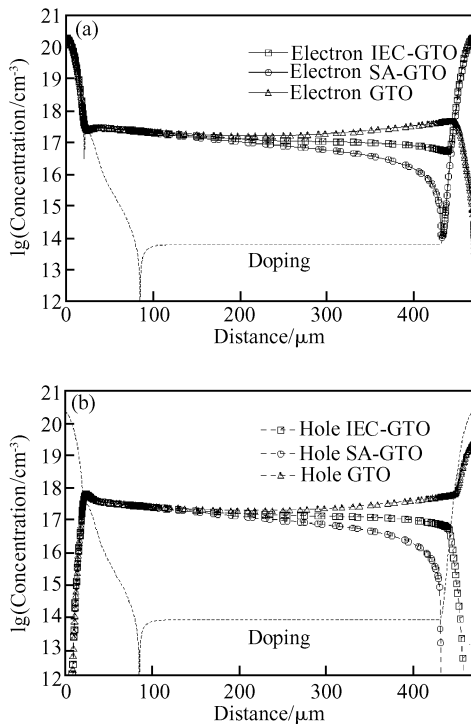


Fig. 3 Comparison of carrier distributions during conduction of IEC-GTO, SA-GTO, and conventional GTO along the profile of  $n^+$  cathode region center (a) Electron concentration distributions; (b) Hole concentration distributions

which the dotted lines express the doping profile. Seen from this figure, the non-equilibrium carrier concentrations in the  $n^-$  base region near the cathode region in the three GTO devices during conduction are close, but near the anode region are different, and the carrier concentration of the conventional GTO is the highest and that of the SA-GTO is the lowest. For the IEC-GTO, the hole concentration in the  $n^+$  floating region is higher than that of the  $n^+$  short region of the SA-GTO, as shown in Fig. 3(b). This shows that the hole IE-effect indeed exists in the IEC-GTO, which is helpful to on-state characteristic. The lower carrier concentration near the anode is helpful to turn-off.

Secondly, a comparison of the  $I$ - $V$  characteristics of the IEC-GTO, SA-GTO, and conventional GTO during conduction is shown in Fig. 4. Seen from this figure, the on-sate characteristic of the IEC-GTO is between that of the SA-GTO and conventional GTO. It is close to that of the conventional GTO at low current density and then increases with the current density. This shows that the IEC-GTO has better on-state characteristics than the SA-GTO.

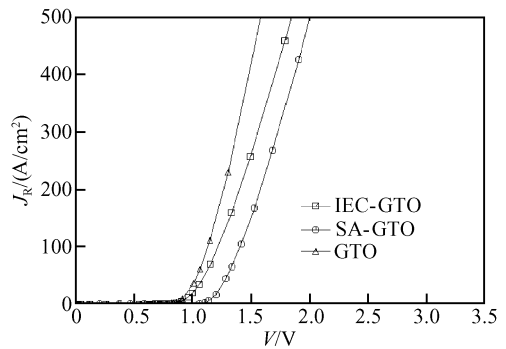


Fig. 4 Comparison of the  $I$ - $V$  characteristics of IEC-GTO, SA-GTO, and conventional GTO during conduction

### 3.3 Switching

Firstly, a comparison of variations of the anode injection efficiency with  $J_A$  of the IEC-GTO, SA-GTO, and conventional GTO during turn-on is shown in Fig. 5, in which hole injection efficiency,  $\gamma_p$  (solid line), and electron injection efficiency,  $\gamma_n$  (dashed), can be expressed by  $J_p/J_A$  and  $J_n/J_A$ <sup>[5]</sup>, respectively, and  $J_A = J_n + J_p$ , i. e.  $\gamma_p + \gamma_n = 1$ . Seen from this figure, when  $J_A < 140 \text{ A/cm}^2$ ,

the  $\gamma_p$  of the conventional GTO is highest, and  $\gamma_p \rightarrow 1, \gamma_n \rightarrow 0$ ; the  $\gamma_p$  of the SA-GTO is lowest, but the  $\gamma_p$  of the IEC-GTO is between them; and when  $J_A > 140 \text{ A/cm}^2$ , the  $\gamma_p$  of the IEC-GTO is even lower than that of the SA-GTO. This is because the  $p^+$  anode region concentration is far higher than that of the  $n^-$  base region in a conventional GTO, resulting in  $J_p \gg J_n$ , and  $\gamma_p \rightarrow 1, \gamma_n \rightarrow 0$ . But the  $n^+$  short region in the SA-GTO enables  $J_n$  to increase and  $J_p \ll J_n$ , so  $\gamma_p \ll 1, \gamma_n \gg 0$ . For the IEC-GTO, when the  $J_A$  is very small, the  $\gamma_p$  of the IEC-GTO is determined by the pnp1, and satisfies  $J_p \gg J_n$ , so  $\gamma_p \approx 1$ . When the  $J_A$  is very high,  $\gamma_p$  is determined by the pnp2, and  $\gamma_p < 1$ . This shows that  $\gamma_p$  of IEC-GTO varied with  $J_A, \gamma_h$  is higher at lower  $J_A$ , but  $\gamma_e$  is higher at higher  $J_A$ . This case is very similar to the GCT<sup>[6]</sup>.

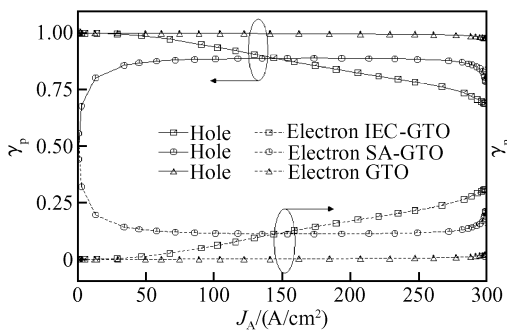


Fig.5 Comparison of the injection efficiency varied with  $J_A$  of IEC-GTO, SA-GTO and conventional GTO during turn on

Secondly, a comparison of the turn-off waveforms of the IEC-GTO, SA-GTO, and conventional GTO under the same gate trigger condition is shown in Fig. 6. Seen from this figure, the variations of anode current and voltage of the IEC-GTO with time is slower than that of the SA-GTO, but quicker than that of the conventional GTO. This is because, when the devices turn-off under the high  $J_A$ , the non-equilibrium electrons stored in the  $n^-$  region in the SA-GTO during conduction can directly reach the anode electrode by low resistance path of the  $n^+$  short region, but the electrons in the conventional GTO can disappear only by recombination, and  $\gamma_p$  under high  $J_A$  is higher. For IEC-GTO, due to a thin oxide layer located at the anode, these electrons cannot be collected directly by the anode contact, so partial electrons still accumulate in the  $n^+$  floating region

near the oxide layer by external voltage except recombination with the holes injected from the  $p^+$  anode region, and  $\gamma_p$  under high  $J_A$  is lower. This enables electrons in the  $n^-$  base region in IEC-GTO to disappear quickly, and the main junction resumes blocking quickly.

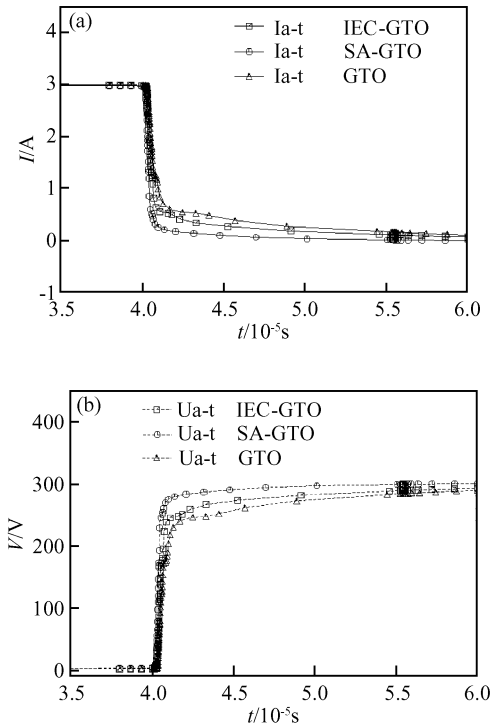


Fig.6 Comparison of the turn-off characteristics of IEC-GTO, SA-GTO, and conventional GTO (a) Variation of anode current with time; (b) Variation of anode voltage with time

### 3.4 Optimization

In order to obtain a better trade-off relation of the characteristics of the IEC-GTO, the surface concentration of the  $p^+$  anode region  $N_{AS}$  and the width of the oxide layer on  $p^+$  anode region  $W_{ox}$  are optimized. The influences of  $N_{AS}$  and  $W_{ox}$  on on-state characteristic and injection efficiency are shown in Fig. 7 and Fig. 8, respectively. Seen from the two figures,  $N_{AS}$  is lower and  $W_{ox}$  is wider, and the on-state characteristic is worse; but  $\gamma_p$  is decreased more at higher  $J_A$ , and the turn-off characteristic is better. This is because the intensity of the hole IE-effect and  $\gamma_p$  are related to  $W_{ox}$  and  $N_{AS}$ , in particular  $N_{AS}$ . Thus the chosen of  $N_{AS}$  and  $W_{ox}$  should consider simultaneously the on-state and turn-off characteristics. Based on the above analysis,  $N_{AS}$  and  $W_{ox}$  can be chosen to be about

$(3\sim 5) \times 10^{18} \text{ cm}^{-3}$  and  $25\mu\text{m}$ , respectively.

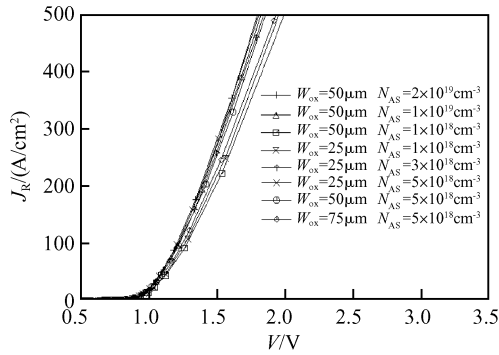


Fig. 7 Influence of the  $N_{AS}$  and  $W_{ox}$  on the on-state characteristic of IEC-GTO

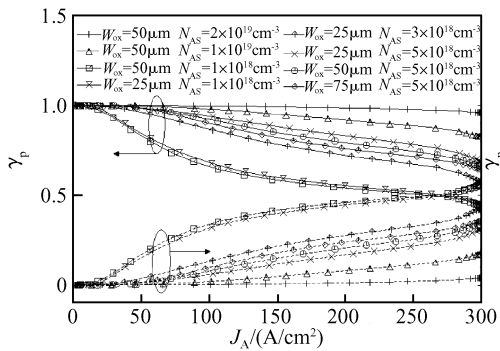


Fig. 8 Influence of the  $N_{AS}$  and  $W_{ox}$  on the anode injection efficiency of IEC-GTO

Additionally, the analysis shows that the influence of the thickness of the oxide layer  $Z_{ox}$  on the characteristics of the IEC-GTO is smaller. In view of physical processes  $Z_{ox}$  is smaller, the required time to form the thinner oxide layer at high temperature is shorter, and the influences on other characteristics of the IEC-GTO are smaller. Thus  $Z_{ox}$  should be chosen to be as thin as possible, about  $0.5\sim 1\mu\text{m}$ .

## 4 How to realize

Based on the above optimized result, in view of physical processes,  $W_{ox}$  and  $Z_{ox}$  can be chosen to be the minimum of photolithography feature size and the thickness of the conventional mask film in physical processes, respectively, so that the thin oxide layer located in the anode of the IEC-GTO has no use for accurate control. At present, the manufacture process of an SA-GTO structure is very mature, and it is fully suitable for the IEC-

GTO. Thus the IEC-GTO structure can be realized by modifying the following based on the process of an SA-GTO.

Firstly, the lower anode doping concentration can be obtained by varying the proportion of impurity solution; Secondly, the anode oxide layer and ohm contact hole can be formed simultaneously with that of the cathode by a dual-side photolithography step; finally, the alloying process can be realized by RTP after aluminum evaporation, and encapsulation can use a press pack. The process of the IEC-GTO is very simple and feasible compared with the GCT<sup>[7]</sup>. This shows that the IEC-GTO not only can improve the characteristics of device, but also has a simpler process similar to the SA-GTO, and the introduction of the oxide layer hardly increases the process complexity.

## 5 Conclusion

A new IEC-GTO structure based on an SA-GTO structure is presented, and its anode injection efficiency can be self-adjusted by its own current and is similar to a GCT. Compared with an SA-GTO and conventional GTO, the IEC-GTO can introduce the hole IE-effect and obtain trade-off relations of on-state and turn-off characteristics. The optimal results show that the additional oxide layer hardly increases the complexity of the manufacture process. It makes the IEC-GTO device very suitable for high-power applications.

## References

- [ 1 ] Gruening H E, Zuckerberger A. Hard drive of GTOs; better switching capability through improved gate-units. IEEE IAS, 1996: 1474
- [ 2 ] Carroll E, Klaka S, Linder S. IGCTs: a new approach to high power electronics. Milwaukee, WI USA: Proceedings of the IEEE International Electric Machines and Drives Conference, 1997
- [ 3 ] Ninomiya H, Takahashi J, Sugiyama K, et al. 4500V trench IEGTs having superior turn-on switching characteristics. ISPSD, 2000: 221
- [ 4 ] Medici Two-Dimensional Device Simulation Program, Version 4.0 User's Manual (AVANT), 2000
- [ 5 ] Benda V, Gowar J, Grant D A. Power semiconductor device theory and application. England: John Wiley & Sons, 1999: 58
- [ 6 ] Wang Cailin, Gao Yong, An Tao, et al. Characteristics analysis of transparent anode GTO. The 4th International Power Electronics and Motion Control Conference, Xi'an, China,

2004;338  
[7] Wang Cailin, Gao Yong, Ma Li, et al. Analysis of mechanism and characteristic for the transparent anode in gate commu-

tated thyristors. *Acta Physica Sinica*, 2005, 54(5): 2296 (in Chinese) [王彩琳, 高勇, 马丽, 等. 门极换流晶闸管透明阳极的机理与特性分析. *物理学报*, 2005, 54(5): 2296]

## 一种新颖的注入效率可控的门极可关断晶闸管的特性分析与优化\*

王彩琳<sup>†</sup> 高 勇

(西安理工大学电子工程系, 西安 710048)

**摘要:** 在阳极短路型门极可关断晶闸管(SA-GTO)的基础上,提出了一种新颖的注入效率可控的门极可关断晶闸管(IEC-GTO),其注入效率可通过一层位于阳极短路接触区的薄氧化层来控制.模拟了 IEC-GTO 的正向阻断、导通和开关特性,并与短路阳极和普通阳极 GTO 的特性进行比较分析.结果表明,IEC-GTO 在关断特性和通态特性间获得较好的折中.最后,通过对薄阳极氧化层宽度和阳极掺杂浓度的优化,分析了工艺的可行性,给出了工艺方案,说明引入氧化层并不会增加 IEC-GTO 的工艺难度.

**关键词:** 电力半导体器件; 门极可关断晶闸管; 注入效率

**EEACC:** 2560P; 2560L; 2560B

**中图分类号:** TN34      **文献标识码:** A      **文章编号:** 0253-4177(2007)04-0484-06

\* 西安理工大学优秀博士生科研基金和科研计划资助项目

<sup>†</sup> 通信作者. Email: wangcailin@xaut.edu.cn

2006-09-28 收到, 2006-11-17 定稿